

Combined Vision and Wearable Sensors-based System for Movement Analysis in Rehabilitation

Sofija Spasojević^{1,2,3}; Tihomir V. Ilić⁴; Slađan Milanović⁵; Veljko Potkonjak¹; Aleksandar Rodić²; José Santos-Victor³

¹School of Electrical Engineering, University of Belgrade, Belgrade, Serbia;

²Mihailo Pupin Institute, University of Belgrade, Belgrade, Serbia;

³Institute for Systems and Robotics, Instituto Superior Técnico, Universidade de Lisboa, Lisbon, Portugal;

⁴Department of Neurophysiology, Medical Faculty of Military Medical Academy, University of Defense, Belgrade, Serbia;

⁵Institute for Medical Research, Department of Neurophysiology, University of Belgrade, Serbia

Keywords

Rehabilitation, movement analysis, Kinect, wearable sensors

Summary

Background: Traditional rehabilitation sessions are often a slow, tedious, disempowering and non-motivational process, supported by clinical assessment tools, i.e. evaluation scales that are prone to subjective rating and imprecise interpretation of patient's performance. Poor patient motivation and insufficient accuracy are thus critical factors that can be improved by new sensing/processing technologies.

Objectives: We aim to develop a portable and affordable system, suitable for home re-

habilitation, which combines vision-based and wearable sensors. We introduce a novel approach for examining and characterizing the rehabilitation movements, using quantitative descriptors. We propose new Movement Performance Indicators (MPIs) that are extracted directly from sensor data and quantify the symmetry, velocity, and acceleration of the movement of different body/hand parts, and that can potentially be used by therapists for diagnosis and progress assessment.

Methods: First, a set of rehabilitation exercises is defined, with the supervision of neurologists and therapists for the specific case of Parkinson's disease. It comprises full-body movements measured with a Kinect device and fine hand movements, acquired with a

data glove. Then, the sensor data is used to compute 25 Movement Performance Indicators, to assist the diagnosis and progress monitoring (assessing the disease stage) in Parkinson's disease. A kinematic hand model is developed for data verification and as an additional resource for extracting supplementary movement information.

Results: Our results show that the proposed Movement Performance Indicators are relevant for the Parkinson's disease assessment. This is further confirmed by correlation of the proposed indicators with clinical tapping test and UPDRS clinical scale. Classification results showed the potential of these indicators to discriminate between the patients and controls, as well as between the stages that characterize the evolution of the disease.

Conclusions: The proposed sensor system, along with the developed approach for rehabilitation movement analysis have a significant potential to support and advance traditional rehabilitation therapy. The main impact of our work is two-fold: (i) the proposition of an approach for supporting the therapists during the diagnosis and monitoring evaluations by reducing subjectivity and imprecision, and (ii) offering the possibility of the system to be used at home for rehabilitation exercises in between sessions with doctors and therapists.

Correspondence to:

Sofija Spasojević
Mihailo Pupin Institute
Volgina 15
11060 Belgrade
Serbia
E-mail: sofija.spasojevic@pupin.rs

Methods Inf Med 2017; 56: ■–■
<https://doi.org/10.3414/ME16-02-0013>
received: March 6, 2016
accepted in revised form: October 22, 2016
epub ahead of print: ■■■

Funding

This work is partially funded by the Ministry of Education, Science and Technology Development of the Republic of Serbia under the contracts TR-35003, III-44008, III-44004 and #ON175012. This work was partially funded by the EU Project POETICON++ and the Portuguese FCT Project [UID/EEA/50009/2013]. The work is complementary supported by the Alexander von Humboldt project „Emotionally Intelligent Robots – Elrobots”, Contract no. 3.4-IP-DEU/112623.

1. Introduction

Traditional rehabilitation techniques for Parkinson's disease (hereinafter, PD) [1] assessment are based on clinical assessment

tools and evaluation scales, such as Hoehn and Yahr (HY) [2] and Unified Parkinson's Disease Rating Scale (UPDRS) [3]. Those scales are descriptive (qualitative) and only the doctor can assess them. Over the past

years, progress in data-analysis and sensing technologies [4] opened new possibilities for improving conventional rehabilitation practice. However, introducing novel technologies into medical protocols is still

challenging, mainly due to: (i) high equipment cost; (ii) system complexity and reliability; (iii) need for a technical support during therapy sessions; (iv) lack of correlation between clinical and technical performance indicators and (v) lengthy and arduous process to obtain the clinical licenses.

Marker-based motion capture (mocap) systems [5] are often used for movement acquisition during rehabilitation sessions, because of their ability to deliver accurate measurements, in spite of their extremely high costs. Other alternatives include the attachment of different sensors to the patient's body [6, 7] or hand (data glove) and, more recently, low-cost marker-free mocap systems such as the Kinect and Xtion [8–10]. The performance of lower-cost systems has been tested and shown to possess a satisfactory accuracy for the application in the rehabilitation therapy [10–13]. While some examples of Kinect-based rehabilitation systems are described in [14–17], little attention has been devoted to the specific case of PD [18, 19]. Recently, authors in [18] have studied the Kinect accuracy for measuring movements of Parkinson's patients, but they did not implement automatic movement analysis. They compared the Kinect to the VICON mocap system through a set of rehabilitation exercises. Their results suggest similar temporal accuracy between the two systems when measuring the movement duration and spatial accuracy regarding the upper body movements. Their general conclusion is that the Kinect has the potential to be used for movement analysis in PD and a promising application in the future for home rehabilitation. To raise the patient's motivation during therapy, some studies have introduced virtual environments into data acquisition and processing procedures for PD [19, 20]. The main limitations with the use of virtual environments and rehabilitation games are the lack of official safety-evidence and proof of clinical effectiveness.

Our previous study [21] introduced an approach for full-body movement analysis (gait and large-range upper body movements) based on Kinect data (3D coordinates of the skeleton joints) to support diagnostic evaluations in PD. However, a full assessment of the PD requires more sophisticated measurements, such as fine

hand movements. Consequently, we have extended our previous work with hand movement analysis, based on the sensory information provided by a data glove, to support the monitoring of PD.

In recent years, various types of wearable sensors have been developed and proposed for measuring and evaluating hand movements: accelerometers [22–24], gyroscopes [25, 26], magnetic sensors [27–29], force sensors [30, 31] and inertial sensors [32]. These sensor systems can only modestly contribute to the hand movement assessment. Specifically, the use of one or two isolated sensors in motion acquisition limits the movement quantification, due to the limited amount of the collected data. Data gloves address this shortcoming by integrating multiple sensors in one single, more sophisticated, device. Most data glove-based systems have a wired connection between the glove and the PC for storing data, which can interfere with the patient's motion and degrade their comfort [33–36]. A wireless system, with five sensors embedded in the data glove is examined in [30]. However, that study is very limited by the low number of sensors for hand movement analysis and omission of the finger joint motion tracking.

Rehabilitation studies for neurological disorders usually focus on the analysis of particular body functionalities, such as postural control [19], gait [37, 38], upper body movements [39] or even the observation of a specific joint [40]. Our work incorporates both the analysis of the full-body functionalities, and hand movements. After acquired sensor data, the next challenge consists in defining suitable features that can be used to characterize the movements in the different subject conditions. We denote such features as *Movement Performance Indicators* (hereinafter, MPIs) for assisting both diagnosis and monitoring. The MPIs we propose build upon domain-specific knowledge provided by doctors and therapists as well as data analysis. Amongst others, we propose a new MPI for upper body rehabilitation, the symmetry ratio, widely used as a validity criterion for models in biomechanics and motor control [41, 42]. In fact, it has been shown that the symmetry of kinematic speed profiles is an exclusive result of neurological mechan-

isms [43, 44], without any interference from changes of conditions or variables of the performed task.

For the hand movement assessment, we have used the wireless Cyber Glove II, a device with eighteen sensors that output joint angular data [45]. Although this system is relatively costly, we have tested it in this study as a proof of concept, towards the design of an affordable version of this data glove for application in the rehabilitation practice. To the best of our knowledge, there are no studies using the Cyber Glove II for quantification of hand movements in PD assessment [46]. We thus propose an affordable, reliable and portable sensor system along with an approach for analyzing a patient's movement, with the potential to be used as a support for the conventional rehabilitation therapy (both during diagnosis and progress monitoring) and home rehabilitation. In addition to symmetry ratio in upper body movements, we propose new hand MPIs, extracted from the data glove sensor signals (abduction sensor data) and the developed hand model (velocity and acceleration parameters).

2. Methods

2.1 Proposed System Structure

► Figure 1 shows the block diagram of the proposed rehabilitation system. The architecture is general, but in our experiments, we have used a Kinect sensor and a data-glove for measuring full-body/fine-hand movements respectively, as detailed in the following paragraphs.

The Kinect is a low-cost motion sensing device that offers a suitable alternative to more expensive and complex vision-based motion capture systems, used today in the rehabilitation practice. The process of the data acquisition is based on the visual skeleton tracking and collecting the 3D positions of characteristic joints without markers. The maximum frame rate for the Kinect is 30 frames per second (30 Hz), but in our case due to additional processing required by data collection, the frame rate drops down to 27 Hz. The acquired data consist of 3D positions of characteristic skeleton joints, along with RGB and depth video sequences (► Figure 2).

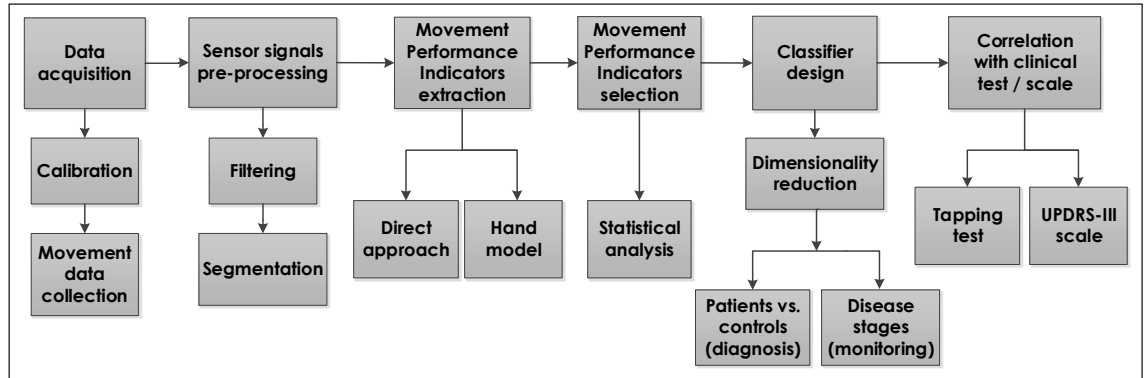


Figure 1
Proposed rehabilitation system structure.

The Cyber Glove II is a wireless, lightweight data glove, adaptable for different hand sizes and suitable for inclusion in rehabilitation protocols. The manufacturer's technical documentation reports sensor data rate up to 90 Hz and repeatability of 3 degrees. The glove has eighteen sensors

giving joint-angle output – metacarpal and proximal sensors on each finger, four abduction sensors between each two consecutive fingers, wrist yaw and wrist pitch sensor placed on the hand wrist and sensors for measuring thumb crossover and palm arch (see ► Figure 3e).

The Kinect device is calibrated by performing a specific calibration body pose. The calibration procedure for the data glove consists of a predefined set of exercises to adjust initialization parameters. As a second stage, the sensor signals are pre-processed with low-pass filters aiming at

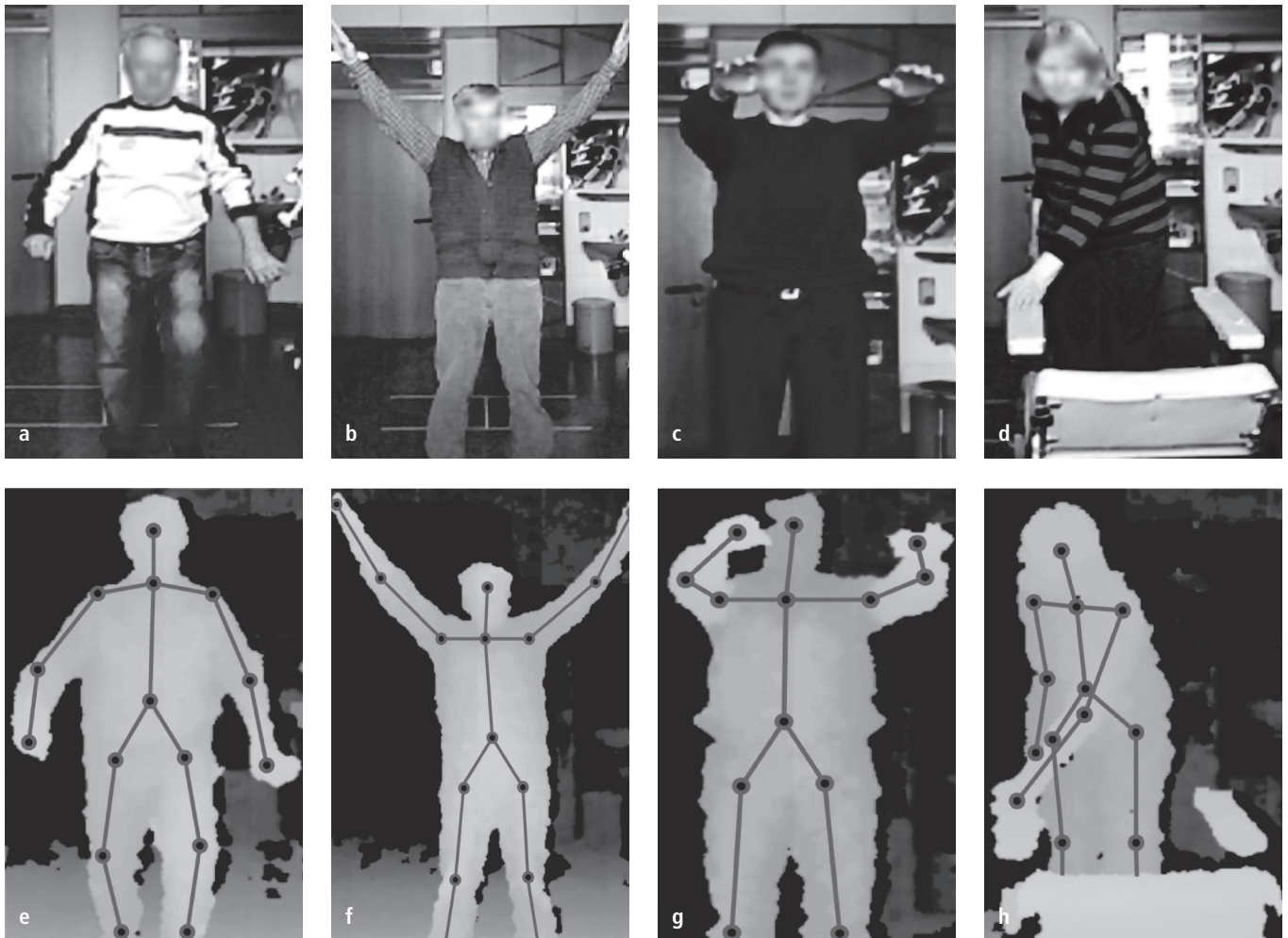


Figure 2 RGB stream (a–d) and depth stream from Kinect with detected skeleton and collected joints (e–h).

reducing measurement noise. A temporal segmentation algorithm is applied to the Kinect sensor signals since the movements are collected in the sequence, but each movement has to be analyzed separately. The MPIs design is detailed in Section 2.3. For characterizing the movements, two approaches have been developed: (i) direct extraction of MPIs from the sensors' signals and (ii) using a hand model to extract indirectly MPIs from the model, explained in a more detail in Section 2.3.2. All proposed MPIs are statistically tested in distinguishing between groups of interest (patients/controls and the first three disease stages according to Hoehn and Yahr (HY) [2]) in the procedure to select the MPIs. The patients at advanced stages of PD (IV/V modified HY scale) are not able to participate in the experiments or wear the sensors, due to the severe motor impairments and functional handicaps. In addition, the movement quantification and inclusion of sensor measurements as a support to clinical evaluations are more of interest in the earlier disease stages. Classifiers are designed as decision-making systems to support diagnosis and monitoring evaluations. Finally, correlation analysis between our proposed MPIs and clinical test/scale has been performed.

2.2 Experimental Procedure

2.2.1 Data Acquisition

The experimental group consists of thirty PD patients with personal and disease characteristics listed in ►Table 1. Patients participated in one, two or all three tests: Kinect and data glove-based tests and clinical tapping test. The number of patients per tests is also listed in ►Table 1. A control group is formed by twenty-three subjects without any history of neurological or movement disorder. All subjects have been examined under the same conditions and they have performed full-body and hand movements, instructed by a neurologist and therapists. The experimental exercises (►Figures 2 and 3) are well-known in the rehabilitation practice, wherein the hand movement analysis is particularly relevant for the evaluation of PD symptoms such as tremor, rigidity, and bradykinesia [1, 3]. Patients receive the daily L-dopa dosage, as well as other anti-PD drugs (►Table 1). All sensor measurements from patients were collected under the effect of medications (ON state).

Following the therapist advice, all rehabilitation exercises are designed to recover or enhance one of the three main human functionalities – balance, mobility in the

sense of normal gait and upper body movements [47]. The gait test is fairly present in the majority of rehabilitation procedures and it can have different forms depending on the equipment used and the measured gait performance indicators/features [47].

In our work, the gait test is carried out in accordance with the available Kinect range [12], with the starting and end points placed at 3.5m and 1.5m away from the Kinect, respectively. During the gait test, patients walked the selected distance of 2m six times with normal and natural gait rhythm (►Figure 2a). The rest of the tested exercises belong to a group of upper body movements: adjusted shoulder abduction-adduction (SAA) (►Figure 2b) until maximum possible range of motion, shoulder flexion-extension (SFE) (►Figure 2c) and movements of the right-left hand between the boundaries (further, hand boundary movements (HBM), ►Figure 2d). The first two exercises were repeated five times, while the HBM was repeated ten times with each hand within experiment.

The set of hand exercises includes finger-tapping movement (►Figure 3a), fingers flexion and extension movement (►Figure 3b), rotation of the hand (►Figure 3c), and fingers expansion and contraction movement (►Figure 3d).

We investigated the correlation between the proposed MPIs, across patients with different disease stages (according to HY scale), and clinical tests – such as tapping test, and UPDRS clinical scale – to assess if such measurements can be used as rehabilitation features.

The clinical measurements (HY and UPDRS) are collected by one experienced rater, immediately before the sensor measurements. All measurements have been performed in the hospital settings for outpatients. The clinician was present during the sensor measurements in order to monitor the patient state, and to prevent situations in which the patient is quickly switched from ON (the effect of medication present) to OFF state (the effect of medication stopped), due to which the possible clinical measurement and sensor measurement would be carried out under different conditions. The Hoehn and Yahr (HY) clinical values (which

| | Total sample (n = 30) | |
|--|------------------------|----------|
| Age (years), mean (SD) Range | 63.57 (8.27) 47–83 | |
| Gender, number of patients (%) | Males | 24 (80%) |
| | Females | 6 (20%) |
| Modified Hoehn & Yahr stage, mean (SD) Range, 1–5 | 2.2 (0.76) 1–3 | |
| UPDRS motor score (section III), mean (SD) Range, 0–108 | 32.08 (11.13) 13–57 | |
| Duration of PD (years), mean (SD) | 4.93 (3.95) | |
| Time on L-dopa (years), mean (SD) | 4.21 (3.20) | |
| Daily L-dopa dosage (mg), mean (SD) | 391.67 (185.72) | |
| Total daily anti-PD dosage (mg), mean (SD) | 725.62 (356.53) | |
| Performed tests, number of patients per test | Kinect | 6 |
| | Data glove | 9 |
| | Data glove + tapping | 9 |
| | All three tests | 6 |

Table 1
Main demographic and clinical characteristics of the patients and performed tests.



Figure 3 Experimental exercises (a–d) and sensor positions on the glove (e).

2.2.2 Data Preprocessing: Noise Filtering and Temporal Segmentation

Data pre-processing is required for noise removal as well as for temporal segmentation (only Kinect data). We have applied Butterworth low-pass filters with cut-off frequency of 3 Hz to raw sensor signals that proved to be effective in terms of noise removal.

Sensor motion data are collected in a sequence of several consecutive repetitions of the instructed movement. Since the MPIs for Kinect data are extracted from each movement separately, a temporal segmentation algorithm is applied to divide the sequence into the corresponding movement segments. On the other hand, the data glove MPIs are extracted at a time for all movements in the sequence; hence segmentation algorithm is applied only to the Kinect data.

The segmentation algorithm is based on the analysis of the relevant joint for each specific movement and detecting its meaningful positions along the particular axis of

evaluate the disease stage) were assessed using the modified Hoehn and Yahr (HY) Scale [2]. The UPDRS clinical values (which evaluate the motor symptoms) were assessed using the motor part of the Unified Parkinson's Disease Rating Scale (UPDRS) [3].

One group of patients performed tapping test [48] that is frequently used by neurologists to examine hand movements in PD patients. The test consists of the proximal and distal tapping tasks using a specially designed board (►Figure 4) as the one proposed in [48]. The proximal tapping task refers to the alternate pressing of two large buttons located 20 cm apart with the palm of the hand during 30 seconds. The distal tapping task is related to the alternate pressing of two closely located buttons (3 cm apart) with the index finger while the wrist is fixed on the table during 30 seconds. Both tests are repeated twice

for the palm and index finger of the right hand, wherein each test lasts thirty seconds and the subject tries to alternately press the buttons as many times as possible. Since the CyberGlove is designed for the right hand, only patients with the affected right side (side on which PD symptoms are initiated) have been tested with the data glove. In the case of Kinect measurements, both, right and left side affected patients have been considered.



Figure 4 Board for tapping test.

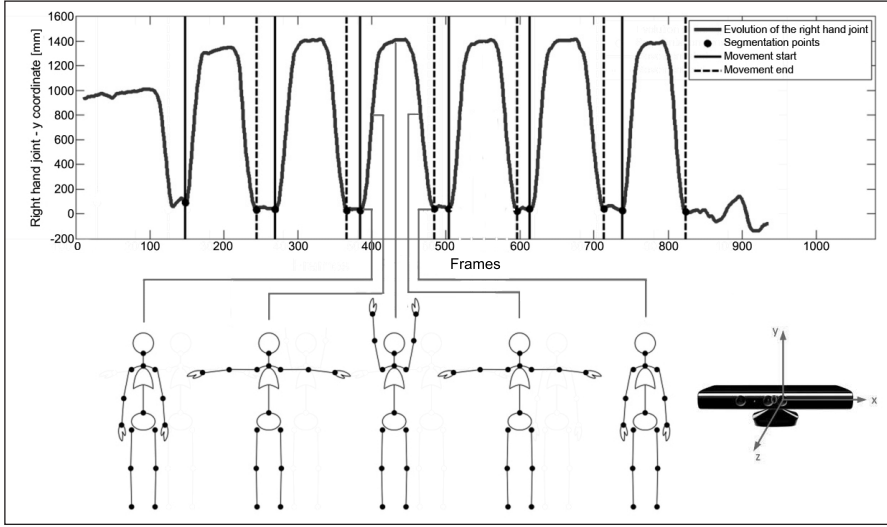


Figure 5 Illustration of the segmentation approach (shoulder abduction movement).

interest. In other words, joint positions can reveal the movement’s starting and termination frames. Let the observed skeleton data be represented by:

$$[J_1, \dots, J_n, \dots, J_N] \in R^{3K \times N}, 1 \leq n \leq N \quad (1)$$

where N is the total number of frames, K is the number of collected joints per frame (K=15) and

$$J_n = [j_1^{v_{n,1}}, \dots, j_k^{v_{n,k}}, \dots, j_K^{v_{n,K}}] \in R^{3K} \quad (2)$$

$$1 \leq k \leq K, j_k^{v_{n,k}} = (x_k^n, y_k^n, z_k^n) \in R^3$$

where J_n represents the set of all K collected joints per frame n and $j_k^{v_{n,k}}$ particular k-th 3D-coordinate joint in the frame n. Our goal is to find a set of vectors (Eq. 3)

$$V = \{[s_1, t_1], \dots, [s_l, t_l], \dots, [s_L, t_L]\}, 1 \leq l \leq L \quad (3)$$

where L denotes the total number of movements (temporal segments) in a sequence and each vector consists of two components: the first one represents the starting frame (s_l) and the second one corresponds to the termination frame (t_l) of the l-th movement.

The segmentation algorithm is based on the search for “peaks” and “valleys” in the input signal, i.e. local maxima or minima. Input signal represents the evolution of the chosen joint in the direction (x, y or z, ►Figure 5) with the most expressed transitions during the particular movement. Under the gait test, it is the evolution of the torso joint in the z-axis direction. As for upper body movements, right-hand joint in the y-axis direction was chosen for shoulder abduction-adduction (►Figure 5) and flexion-extension movement, while the both hand joints in the x-axis direction represent the input signals of the segmentation algo-

rithm for hand boundary movement sequence. Segmentation points are extracted from the determined set of local minima and maxima points. Then, the actual beginning and end of the movements are isolated based on the two types of threshold conditions: (i) amplitude value threshold (amplitude range in which segmentation points lie) and (ii) temporal position threshold (corresponding distance in time between the points of interest must be satisfied). Threshold values are established depending on the particular movement and its temporal evolution in the selected direction.

►Figure 5 illustrates the segmentation algorithm for the case of shoulder abduction-adduction movement sequence. Evolution of the right-hand joint in the y-axis direction shows that y value increases from the starting position in the first part of the movement (when the arms go up) and then decreases in the second part of the movement (when the arms go down). The actual starting and ending points for all six movements in the sequence are correctly determined by our segmentation algorithm (►Figure 5).

2.3 Proposed Approach for Movement Characterization

We have used several MPIs that represent the movements of the different body parts (using the Kinect) or hands (using the data-glove) of a subject. The choice of MPIs was partly resulting from discussions with doctors, therapists, and other domain experts. In the following sections, we will detail how these MPIs were designed.

2.3.1 Full-body Movements

All together we have used 10 different MPIs that result from the combination of four measurement categories (speed, rigidity, the range of motion and symmetry) applied to 4 categories of full-body movements, as illustrated in ►Table 2.

The MPIs we extracted from gait movements are commonly used in the rehabilitation practice and treatment [28]. From gait movements, we considered three MPIs – speed of the gait, variations in the gait speed, and hand rigidity – during walking. We have adopted the mean gait speed V,

Table 2 The proposed MPIs result from a combination of 4 body movements and 4 MPI categories (speed, rigidity, range of motion and symmetry).

| Movements/MPI categories | Speed/Speed variations | Rigidity | Range of Motion (ROM) | Symmetry Ratio (SR) |
|------------------------------------|------------------------------------|------------------|-----------------------|---------------------|
| Gait | MPI ₁ /MPI ₂ | MPI ₃ | | |
| Shoulder abduction-adduction (SAA) | MPI ₅ | | MPI ₄ | MPI ₆ |
| Shoulder flexion-extension (SFE) | MPI ₈ | | MPI ₇ | MPI ₉ |
| Hand boundary movements (HBM) | MPI ₁₀ | | | |

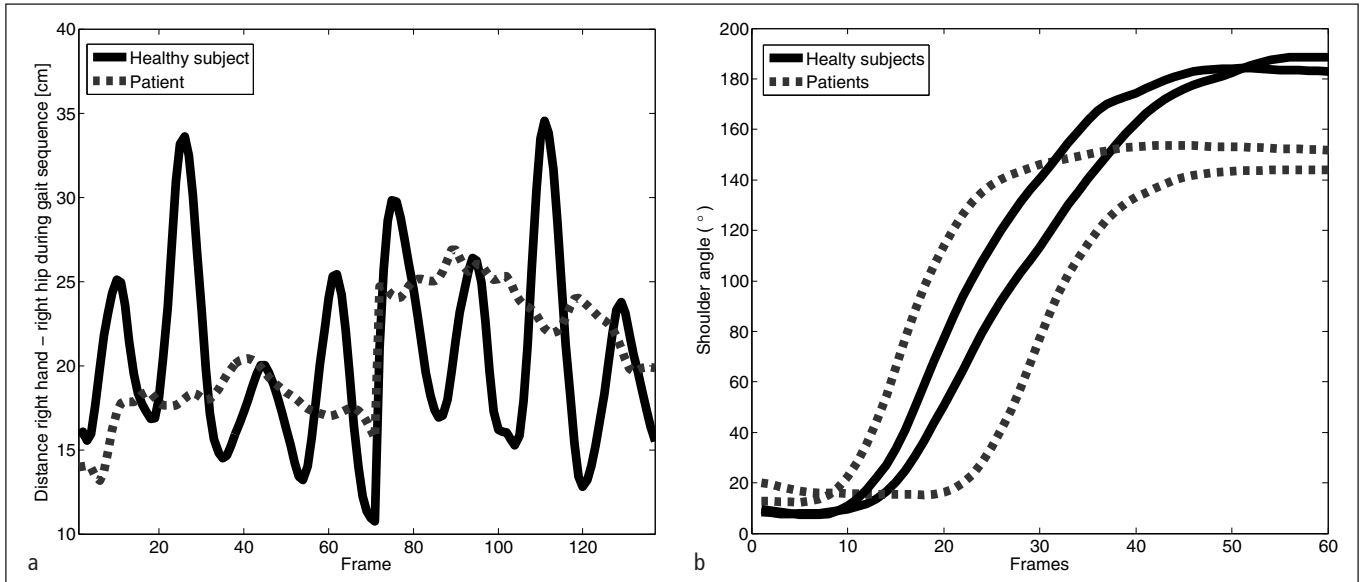


Figure 6 (a) The difference between the left/right hand-hip distances shows the rigidity symptom. (b) Evolution of the shoulder angle profiles during shoulder abduction movements.

Eq. (4), during each two-meter sequence. Due to possible deviations of the starting and end point of the gait test, and in order to improve the accuracy, the path length (the numerator in Eq. (4)) has been calculated as the total trajectory of the torso during each gait sequence, instead of setting the path length of 2m. The total trajectory length is obtained by summing up the Euclidean distances (d) between the torso joint coordinates $X_i(x_i, y_i, z_i)$ and $X_{i-1}(x_{i-1}, y_{i-1}, z_{i-1})$ for consecutive frames, i and $i-1$, during the gait sequence. The time duration of the gait sequence (the denominator in Eq. (4)) is computed based on the total number of frames (m and n denote respectively the first and last frame of the sequence) and the frame rate, $f=27$ Hz.

$$V = \frac{\sum_{i=m}^n d(X_i, X_{i-1})}{(n-m+1)/f} \quad (4)$$

Variations in the gait speed are calculated as the differences in the mean gait speed between consecutive gait sequences within gait test. This MPI can be an indicator of the unbalanced gait if the speed value significantly differs from one gait sequence to another. The position of the arms during walking can reveal rigidity, one of the main indicators of the PD [1]. In the case of healthy subjects, the arms usually swing in

a certain rhythm during gait activity, in contrast to the Parkinson's patients. We have computed a measure of rigidity, based on temporal evolution of the hand position during the gait test. The rigidity symptom can be noticed in the variation of the distance between the hip and hand during the gait sequence. For healthy subjects, the temporal evolution of these distances is approximately periodic, due to normal arm swing. In contrast, for patients with one rigid arm, the distance between the rigid hand and the closest hip does change significantly over time (►Figure 6a). The measure of rigidity is calculated in two steps. First, we record the difference signal between the left and right hand-hip distances, during the gait movement. Then, we take the highest value of the (absolute) difference signal as an indicator of rigidity.

For patients with a rigid arm the difference signal is larger because the healthy arm performs a normal swing and the rigid arm remains more or less static. Instead, healthy subjects display a lower-amplitude difference signal, due to the normal swing of both hands.

Inspired by the well-known and widely used rehabilitation measure for upper body movements, we have also computed the range of motion [47] for the shoulder abduction-adduction and shoulder flexion-extension exercise. The range of motion

represents an angle of the movement relative to a specific body axis, which can be measured at various joints such as elbow, shoulder, knee, etc. In our case, we measure the evolution of the shoulder angle during the movement in relation to the longitudinal body axis.

As a specific MPI, we have used the range of motion (maximum achieved shoulder angle). Examples of the shoulder angle profiles of both normal subjects and patients for the shoulder abduction movement are shown in ►Figure 6b. The range of motion is higher for healthy subjects (more than 180°) than for patients (142°, 150°).

In addition, the trajectory of shoulder angle is steeper for healthy subjects, indicating a higher speed of movement. We calculated the mean movement speed for all three tested upper body exercises. The applied procedure was the same for the gait speed (Eq. 4), setting the path length to the total length of hand trajectory during the movement.

The comparison between relevant left/right body-side movement descriptors can suggest which side or limb is more affected by the neurological disorder. For healthy subjects, these differences are usually negligible, while they can become quite large for Parkinson's patients, depending on the disease stage.

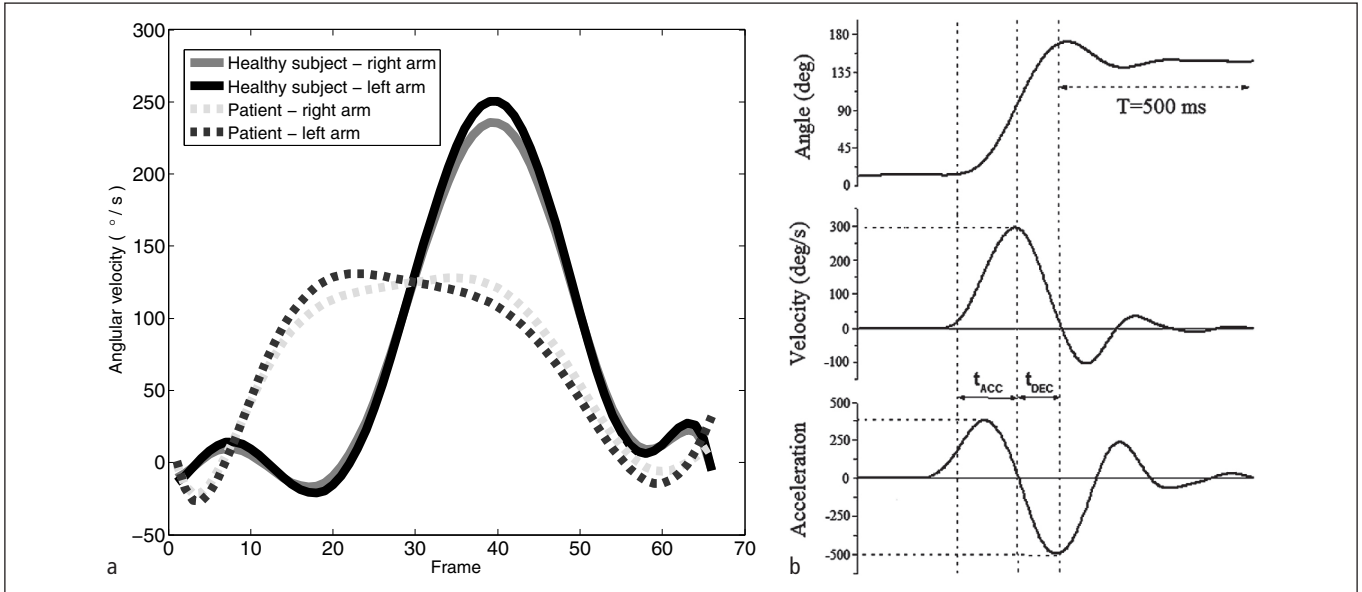


Figure 7 Evolution of the shoulder angular velocity profiles during shoulder abduction movements (a) and symmetry ratio calculation (b).

Important movement descriptors such as profiles of joint angles (► Figure 6b) and angular velocity profiles (► Figure 7a) can reveal the symmetry of the movements. In order to quantitatively assess the movement symmetry, we have extracted symmetry ratio from the shoulder abduction-adduction and shoulder flexion-extension exercises. In motor control, the symmetry

ratio (SR) [41–44] (► Figure 7b) is defined as the ratio between acceleration (t_{ACC}) and deceleration (t_{DEC}) times, during one movement. ► Figure 7a shows that the maximum angular velocity of the shoulder abduction movement is higher for healthy subjects than it is for Parkinson’s patients. In addition, healthy subjects reach the maximum angular velocities of the left/

right arm movements approximately at the same time as opposed to non-healthy subjects, where a difference of about 20 frames is typical. The consequence is unbalance in symmetry ratios between left and right arm for the same movement. Thus, in our experiments, we obtained larger left-right differences of the symmetry ratios for Parkinson’s patients than in healthy subjects.

We have described 10 MPIs extracted from the Kinect data to quantify the movements of different body parts during a rehabilitation session. These MPIs will be used later on to diagnose and characterize the progress of the Parkinson’s patients. In the next section, we will explain how the hand movements were also taken into consideration for a finer analysis.

2.3.2 Hand Movements

Similarly to what we have done for full-body movements, we propose a new set of MPIs to characterize the hand movements (► Table 3) with respect to: (1) range of motion of the characteristic hand and finger joints (for fingers flexion and extension movement and rotation of the hand); (2) velocity values derived from abduction sensor angular data (for finger expansion and contraction movement) and (3) velocity and acceleration parameters between thumb and index finger tips estimated

Table 3 Extracted MPIs from the collected hand movements.

| Movements | Fingers flexion and extension | Hand rotation | Fingers expansion and contraction | Finger tapping movement |
|---------------------|---|--|---|--|
| Extracted MPIs | Joint range of motion Proximal: thumb (MPI ₁₁), index (MPI ₁₂), middle (MPI ₁₃), ring (MPI ₁₄) Metacarpal: index (MPI ₁₅), middle (MPI ₁₆), ring (MPI ₁₇), pinky (MPI ₁₈) | Joints range of motion Wrist yaw (MPI ₂₃) | Angular velocity data Abduction sensors (MPI ₁₉ , MPI ₂₀ , MPI ₂₁ , MPI ₂₂) | Velocity (MPI ₂₄) and acceleration (MPI ₂₅) signal parameters |
| Sensors of interest |  | | | Hand model |

from the hand model (for finger-tapping movement).

The range of motion (ROM) of the hand and fingers characteristic joints can be derived directly from the sensor angular data signals. It is defined as the distance between the angular sensor values from the initial (minimum angular value) to the final position (maximum angular value) during each movement in the sequence (► Figure 8a).

The ROM measurement is extracted from the fingers flexion and extension movement and hand rotation movement. The fingers flexion and extension movement is representative in the investigation of the tremor, dyskinesia and the mobility of the fingers. Subjects are asked to perform twenty consecutive alternating fingers flexion and extension movements as fast as possible. For the quantification of this movement, we concentrate on the sensor data collected from metacarpal (index, middle, ring and little finger) and proximal finger joints (thumb, index, middle and ring finger) according to their high activity during movement performance (► Table 3).

The rotation of the hand movement can indicate the presence and severity of the rigidity symptom. Under this movement's test, subjects need to rotate their hand to the left and right direction alternately as fast as possible during a ten second period. The relevant sensor data for this movement are collected from the wrist yaw position (► Table 3). The angular data profiles of wrist yaw joint (► Figure 8b) for control subjects show the expressed periodicity and wide range of motion. For patients, the range of motion is substantially smaller and the signal clearly illustrates the execution of slower movements (► Figure 8b).

The fingers expansion and contraction movement tests the functionality, flexibility and speed of finger movements; hence, it can reveal the presence of asynchronous, uncoordinated motion and dyskinesia. Subjects are asked to perform ten consecutive fingers expansion and contraction movements. It is characterized using four abduction sensors, placed between each two consecutive fingers. The angular velocity signals are derived from processed angular data since the velocity values have underlined greater differences between ex-

perimental and control group than range of motion data. Maximum angular velocity values for each movement in a sequence of both, expansion (► Figure 9, circles) and

contraction phase (► Figure 9, squares) are extracted as MPIs. Evolution of the angular velocity profiles of patient and control subject for ring-pinky abduction sensor is

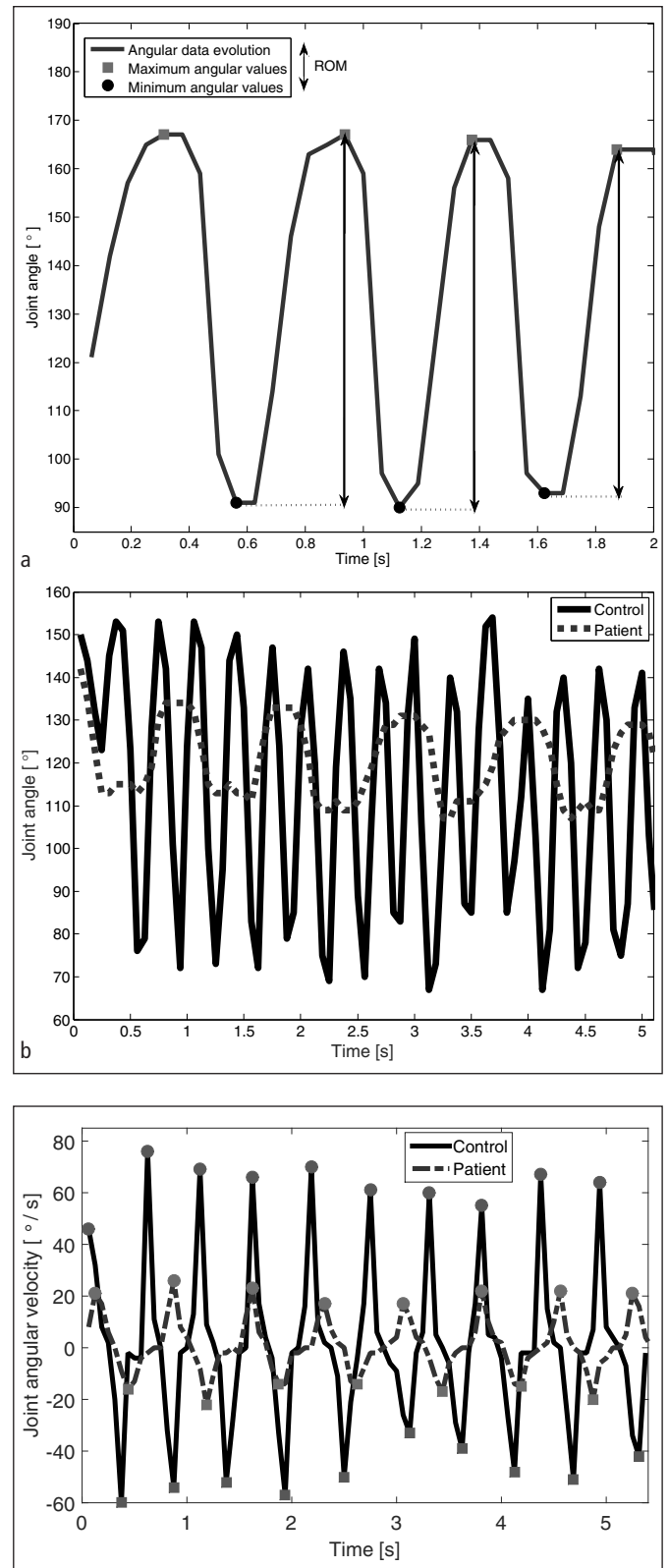


Figure 8 Calculating the range of motion (ROM) of finger joints (a) and evolution of the wrist yaw joint angular data profiles during rotation of the hand movement (b).

Figure 9 Evolution of the abduction sensor (ring-pinky position) angular velocity data profiles during fingers expansion and contraction movement.

given in ▶ Figure 9. It can be seen that control subject's consecutive expansion-contraction finger movements reach higher velocity values compared to the same movements in patients.

2.3.3 Model-based Estimate of Hand MPIs

Finger-tapping movement is the most frequent rehabilitation exercise in the PD protocol, which tests symptoms such as tremor, dyskinesia, and bradykinesia. In our finger tapping test, subjects are directed to perform twenty consecutive touches between the thumb and index finger tips as fast as possible with the elbow fixed on the table. It has been widely studied and some attempts at its quantification are reported in [22, 28, 29, 49]. In some of these approaches, sensors are attached at the thumb and index finger tips making contact detections during the finger-tapping movement performance. In [22, 49] measurement system is composed of two accelerometers, while in [28, 29] magnetic sensors are used. The main drawback of these systems is the analysis of one particular movement since, due to the sensor placement, only the evaluation of the finger-tapping movement is feasible.

Unfortunately, the sensor glove we used does not possess sensors on the fingertips and available joint-angle data are not enough to characterize finger-tapping movement. To overcome this, we developed a hand model and used the model to

estimate the fingertips position information. The hand model allows us to produce estimates of different hand-related measurements (distance, velocity, acceleration), without using specific sensors (e.g. accelerometers) for that purpose. Consequently, our approach provides a comprehensive analysis of several hand movements along with finger tapping movement, without excluding significant sensor information.

The Kinematic hand model with 20 degrees of freedom is fed with the joint-angle data collected by the sensor glove and real dimensions of the subject's finger sections, measured at the time of experiments. Based on this information and using direct kinematics, the positions of the fingertips can be estimated. Every finger is treated as a serial kinematic chain, which is modeled using Denavit-Hartenberg (D-H) representation [50, 51]. As a by-product, the kinematic hand model can be used to visualize the hand movements and check whether the sensor data keep track of real finger movements within the appropriate range of motion.

Finger tapping movement is quantified based on the velocity and acceleration signals. Those signals are obtained as derivatives of the distance information between thumb and index fingertips during finger-tapping movement. Concrete MPI values are represented by the extreme points of the velocity and acceleration signals. ▶ Figure 10 shows the extracted MPIs (marked using circles and squares) during the movement sequence.

2.4 Internal Consistency of the Sensor Measurements and Reliability of the MPIs

We assessed the internal consistency of the sensor measurements using Cronbach's alpha parameter [52]. In the case of the Kinect sensor measurements, Cronbach's alpha parameter was investigated for four recorded movements (▶ Figure 2a–d), fifteen collected joints (▶ Figure 2e–h) and three coordinates (▶ Figure 5) in the sense of the collected patient's data (12 patients in total). All obtained Cronbach's alpha parameters across different movements, joints and coordinates have values within the range [0.91–0.99]. Values of the Cronbach's alpha parameter close to one indicate the high consistency of the Kinect sensor measurements.

Similar analysis has been conducted for the data glove measurements. The Cronbach's alpha parameter was determined for four collected hand movements (▶ Figure 3 a–d) and eighteen sensors placed inside the Cyber Glove (▶ Figure 3e). The data set for internal consistency investigation consists of 24 patients. Our results across different movements and sensor outputs report the values of the Cronbach's alpha parameter within the range [0.86–0.99], and thus, confirm the high consistency of the data glove sensor measurements, as well.

In order to test the reliability of the extracted MPIs, the split-half method for

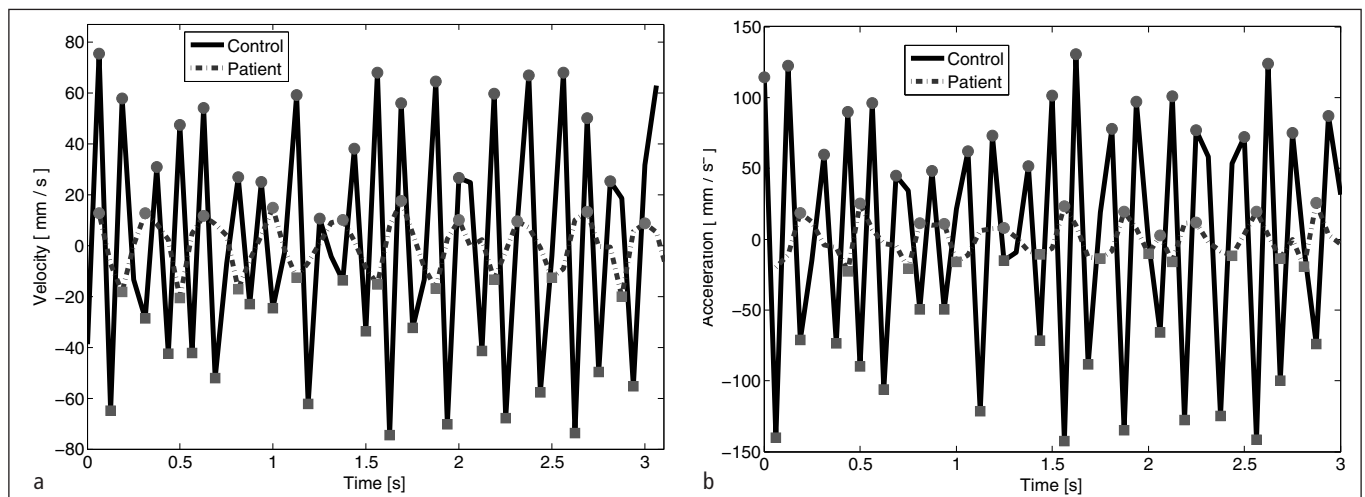


Figure 10 Estimated velocity (a) and acceleration (b) signals from the hand model.

Table 4 ICC reliability parameters of the extracted Kinect and data glove MPIs.

| Kinect MPIs | ICC | 95% CI | Data glove MPIs | ICC | 95% CI | Data glove MPIs | ICC | 95% CI |
|-------------|------|-------------|-----------------|------|---------------|-----------------|------|---------------|
| 1. | 0.94 | [0.89–0.97] | 11. | 0.97 | [0.969–0.979] | 19. | 0.90 | [0.882–0.920] |
| 2. | 0.59 | [0.20–0.79] | 12. | 0.97 | [0.962–0.974] | 20. | 0.92 | [0.898–0.930] |
| 3. | 0.65 | [0.32–0.82] | 13. | 0.98 | [0.971–0.980] | 21. | 0.92 | [0.903–0.934] |
| 4. | 0.96 | [0.92–0.98] | 14. | 0.97 | [0.969–0.979] | 22. | 0.90 | [0.882–0.920] |
| 5. | 0.97 | [0.93–0.98] | 15. | 0.98 | [0.982–0.988] | 23. | 0.97 | [0.964–0.975] |
| 6. | 0.74 | [0.49–0.87] | 16. | 0.98 | [0.983–0.989] | 24. | 0.99 | [0.987–0.998] |
| 7. | 0.81 | [0.62–0.90] | 17. | 0.99 | [0.984–0.989] | 25. | 0.99 | [0.988–0.999] |
| 8. | 0.95 | [0.91–0.98] | 18. | 0.98 | [0.971–0.980] | | | |
| 9. | 0.51 | [0.15–0.75] | | | | | | |
| 10. | 0.92 | [0.84–0.96] | | | | | | |

reliability analysis [52] has been applied. The split-half method divides the conducted tests into two parts and correlates the scores on one-half of the test with scores on the other half of the test. Thus, the split-half method estimates the reliability based on the repetitions inside the same trial. Reliability of the extracted MPIs from the Kinect and data glove data is assessed using Intraclass correlation coefficient (ICC) [52]. Results are shown in the ►Table 4 for both, Kinect and data glove MPIs, along with the 95% confidence intervals. The complete list of the numbered MPIs is given by ►Figures 11 (Kinect MPIs) and 12 (data glove MPIs).

Results of the reliability analysis have demonstrated the high reliability of the data glove MPIs ($ICC \geq 0.90$ for all MPIs). In the case of the Kinect MPIs, the majority of the extracted MPIs have shown the high reliability, except the Variations in the gait speed MPI and the Difference between right and left SR MPI (SFE movement), where the values of ICC are less than 0.60.

3. Results

We have defined a set of 25 MPIs (10 for the full-body and 15 for the hand movements) that can be used both for diagnosis and progress monitoring of PD during rehabilitation. The design of these MPIs was grounded on the information provided by neurologists and therapists with the goal of delivering quantitative information about

subject's performance. In this section, we will show the relationship of these MPIs with the demographic and clinical characteristics of subjects, how these MPIs were selected from the initial MPIs set and how they can be successfully used in practice. We will address both full-body movements captured with the Kinect sensor and fine hand movements measured with the data glove.

When dealing with the initial MPIs set, three important questions are imposed: (1) What is the relationship between the proposed MPIs and the demographic and clinical characteristics of subjects? (2) Which MPIs are the more relevant and informative? (3) Can we improve classification results if we design an optimized MPIs set? To answer the first question we conducted statistical analysis using mixed effect models. To investigate questions 2–3

we adopted a Linear Discriminant Analysis (LDA) approach [53].

3.1 Statistical Evaluation of the MPIs across Demographic and Clinical Parameters

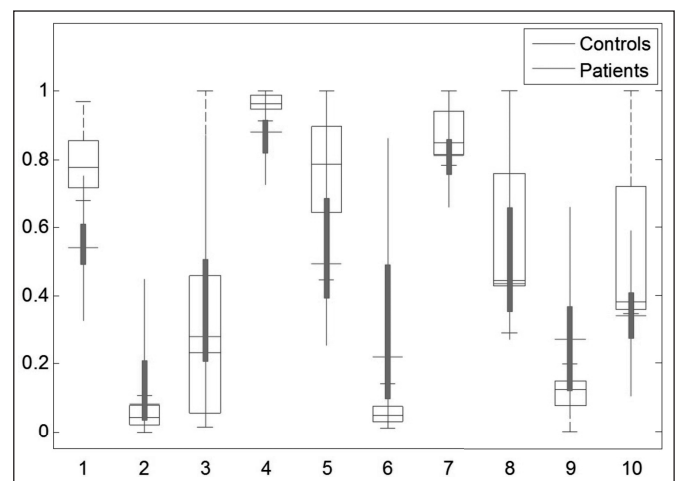
We investigated the relationship between the proposed MPIs and the demographic and clinical characteristics of subjects – age, gender, and clinical group: (i) patients/controls and (ii) disease stage group. In order to reveal whether those characteristics are statistically significantly correlated with the primarily proposed MPIs, we have used mixed effect models [52]. Our initial MPIs set consisted of 30 MPIs (11 full-body and 19 hand movement MPIs).

Every MPI was modeled based on fixed and random effects. As fixed effects, we in-

Figure 11

MPI ranges (Kinect data).

1. Gait speed [m/s]
2. Variations in the gait speed [m/s]
3. Rigidity measure[cm]
4. ROM (SAA) [°]
5. Speed (SAA) [m/s]
6. Difference between right and left SR (SAA)
7. ROM (SFE) [°]
8. Speed (SFE) [m/s]
9. Difference between right and left SR (SFE)
10. Speed (HBM) [m/s]



cluded the age, gender, and group effect. Intra-individual variations in repeated measures were modeled as the random effect. Statistical significance of the fixed effects was assessed by corresponding p-values (5% confidence level) after correction using Benjamini-Hochberg procedure for multiple testing. Mixed effect model fitting was performed for thirty initially proposed MPIs.

The key results of the statistical analysis lead to two main conclusions: (i) the demographic parameters, age, and gender, did not have significant influence ($p \gg 0.05$) on the MPIs and (ii) in addition, five of thirty MPIs had no significant correlation with the clinical group effect ($p > 0.05$). Those MPIs represent one full-body MPI (the measure of tremor) and four hand movement MPIs (ROM of thumb metacarpal joint, ROM of pinky proximal joint, ROM of wrist pitch and distance parameter of the hand model). Hence, as suggested by these statistical studies, the subsequent data analysis (dimensionality reduction, classification, and correlation analysis) was carried out with the clinical group information only (demographic parameters were not relevant) and using the identified 25 MPIs. Such outcomes lead to the simplification in terms of the number of clusters and

data needs and rejection of five MPIs in the subsequent data analysis.

3.1.1 Overview of the Full-body and Hand MPI Value Ranges

► Figures 11 and 12 provide additional insight concerning full-body and hand MPIs, adopted in the previous section and their ranges across patients and controls. Because of their higher values, MPIs 3, 4, 5, 7, 8 and 10 were normalized, in order to allow a comparative representation with other MPIs. The values of the range of motion and gait/movement speed are lower in the patient group, while the left-right arm differences of the symmetry ratio, during shoulder movements, as well as variations in the gait speed, are much larger in patients, as expected.

► Figure 12 illustrates lower values of finger joints range of motion in the patient group, as expected. Our experiments have shown especially large differences in angular velocity values between patients and controls for fingers expansion and contraction movement (► Figure 12, 19–22), as well as in the case of MPIs extracted from the hand model (► Figure 12, 24–25). Hence, the results confirm that our newly proposed MPIs would give significant contribution to support the evaluations in PD.

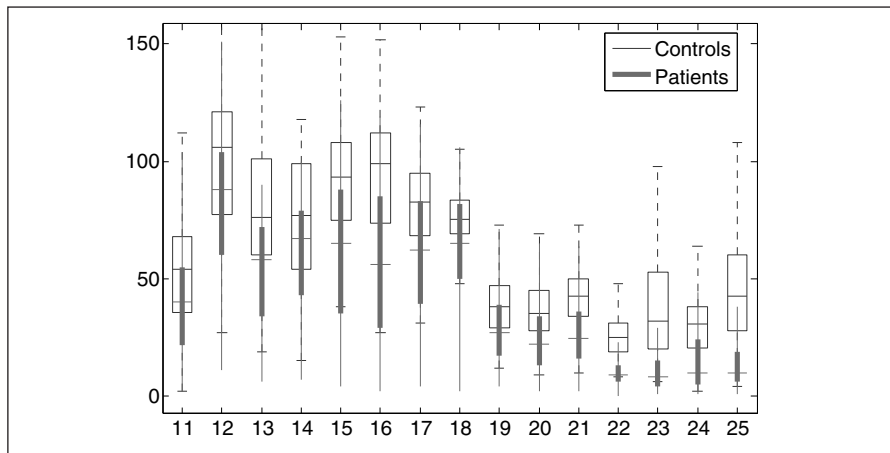


Figure 12 MPI ranges (sensor glove data).
 11. ROM thumb proximal [°]
 12. ROM index proximal [°]
 13. ROM middle proximal [°]
 14. ROM ring proximal [°]
 15. ROM index metacarpal [°]
 16. ROM middle metacarpal [°]
 17. ROM ring metacarpal [°]

18. ROM pinky metacarpal [°]
 19. Angular velocities index-middle adduction [°/s]
 20. Angular velocities middle-ring adduction [°/s]
 21. Angular velocities ring-pinky adduction [°/s]
 22. Angular velocities thumb-index adduction [°/s]
 23. ROM wrist yaw [°]
 24. Velocity hand model [mm/s]
 25. Acceleration hand model [mm/s²]

3.2 Dimensionality Reduction

By adopting the 25 MPIs for the tested full-body and hand exercises, we obtain two sets of 10-dimensional and 15-dimensional feature vectors (► Figure 11 and 12), which can be used in a classification system to assist diagnosis and monitoring. We applied Linear Discriminant Analysis (LDA) [53] to determine the most relevant MPIs for the decision-making process based on the clinical group parameter, between patients and controls (diagnosis support) and between disease stages (monitoring support). Demographic parameters were not of interest according to the statistical analysis described in Section 3.1. Another outcome of the LDA algorithm is the transformation of the MPI data set into a new, compact, lower dimensional space. The LDA approach aims to maximize the between-class distance and to minimize within-class dissipation. The dimension of the newly created space is determined from the eigenvalues of the LDA criterion function, which takes into account the class covariances. Our tests revealed that, both in the 10-dimensional and 15-dimensional feature spaces, the sum of the first two eigenvalues was much larger than the sum of the remaining eigenvalues ($\lambda_1 + \lambda_2 \gg \lambda_3 + \dots + \lambda_m$), where m denotes the total number of features. Hence, both feature sets are reduced to the new 2-dimensional feature space.

As a side-result, the LDA method ranks the original features in terms of their contribution to the reduced feature space based on the weights ($v_{11} \dots v_{m1}; v_{12} \dots v_{m2}$) of the transformation matrix V , where m represents the total number of features, (Eq. 5). S is the matrix of the original data set with n samples while the L represents the matrix of reduced data set to 2-dimensional feature space.

$$L = S * V \Leftrightarrow \begin{bmatrix} l_{11} & l_{12} \\ \dots & \dots \\ l_{n1} & l_{n2} \end{bmatrix} = \begin{bmatrix} s_{11} & \dots & s_{1m} \\ \dots & \dots & \dots \\ s_{n1} & \dots & s_{nm} \end{bmatrix} * \begin{bmatrix} v_{11} & v_{12} \\ \dots & \dots \\ v_{m1} & v_{m2} \end{bmatrix} \quad (5)$$

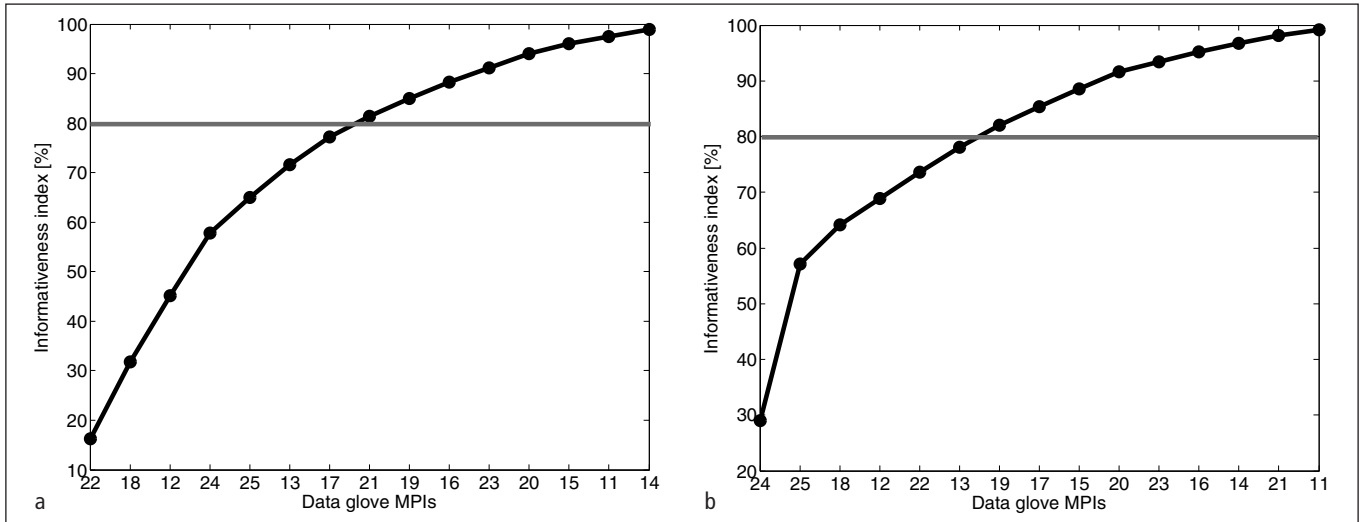


Figure 13 LDA Informativeness index: (a) patients-controls and (b) disease stages data.

The modified Informativeness Index ($II(f)$) based on the weights of the transformation matrix is adopted for the first f features using Eq. (6):

$$II(f) = \frac{\sum_{i=1}^f \text{abs}(v_{i1} + v_{i2})}{\sum_{i=1}^m \text{abs}(v_{i1} + v_{i2})}, \quad 1 \leq f \leq m \quad (6)$$

where the decreasing order of the sum of weights is considered:

$$(v_{11} + v_{12}) \geq (v_{21} + v_{22}) \geq \dots \geq (v_{m1} + v_{m2}).$$

The LDA method for groups of patients and controls results that, for keeping 80% of information from the original Kinect data set, it is sufficient to select the MPIs 1, 6, 9 and 10 from ►Figure 12. This result shows that, in addition to the speed of the gait and upper-body movement (HBM), both symmetry ratio MPIs are amongst the most informative MPIs.

The same criterion, of capturing 80% of the information from the original data sets, is applied to verify the most relevant hand MPIs. Consequently, we have chosen first seven features during LDA analysis for groups of patients and controls and six features from the LDA procedure in the case of disease stages (►Figure 13). MPIs 22, 18, 12, 24, 25, 13 and 17 from ►Figure 12 have the highest contribution to differentiate classes of pa-

tients and healthy-subjects, while MPIs 24, 25, 18, 12, 22 and 13 were the most representative features during dimensionality reduction according to disease stage classes. This result suggests that the MPIs extracted from the hand model are the most relevant features in both cases. In addition, ROM MPIs (fingers flexion and extension movement – both proximal and metacarpal joints) and angular velocity MPIs (fingers expansion and contraction movement – thumb-index abduction sensor), are also very important in the data analysis.

The LDA method also provides us with new synthetic features that form a reduced-dimension feature space. While these new synthetic features have the power to differentiate the different conditions in the data, they are less efficient in terms of communication and understanding for the medical doctors and therapists, as they do not correspond to a specific MPI.

3.3 Classification: Diagnosis and Monitoring Evaluations

So far, we have shown how to build a set of MPIs from the movement of body/hands of Parkinson's patients. Statistical analysis using mixed effect models confirmed the significance of the clinical group factor in relation to MPIs, in contrast to demographic factors that turn out to be non-relevant. In addition, it has underlined 25 MPIs out of 30 as signifi-

cantly correlated with clinical group effect. The LDA analysis has established a new reduced-dimension feature space and determined the most relevant MPIs. In this section, we present a classification approach that can automatically identify the different subject groups (patients/controls and disease stages) based on the original and the derived feature sets. First, we built a classification model using the training data. Second, we adopt the model parameters in the cross-validation procedure. Finally, we test the model on the unseen testing data. This procedure is performed for all classifiers.

Using the Kinect data, we have tested the classification between healthy and non-healthy subjects in three different conditions: (i) with the original feature set, (ii) using the four most relevant features adopted in the previous section and (iii) the two new synthetic features, obtained from LDA. We have compared three different classifiers (►Figure 14): (a) SVM – support vector machines with RBF kernel

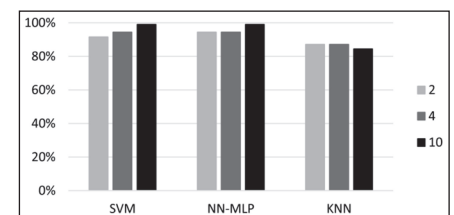


Figure 14 Classification accuracy of Kinect data (patients/controls).

(bandwidth of the RBF kernel, σ and regularization parameter, C : $0.01 < \sigma < 1$, $0.01 < C < 10$), (b) KNN (number of nearest neighbors, $k \in 1, 3, 5$) and (c) neural networks (MLP – multilayer perceptron: various structures with different number of hidden layers and nodes). The parameters of classifiers were chosen from above specified ranges in a validation procedure in order to achieve the highest accuracy rate. ► Figure 14 shows that all classifiers succeed to differentiate healthy from non-healthy subjects. The SVM and the NN-MLP have the best results when using the original feature set. The KNN classifier works best for the reduced feature sets but in general, is the least performing classifier. We achieve classification results close to 100% on the unseen testing samples, compared to the chance level of 50%.

The Kinect data showed poor results during classification between the disease stages. We achieved a classification accuracy of about 50%, compared to the chance level of 33%, which is not enough for evaluating the disease stage. Our results show that, while the Kinect MPIs have the power to distinguish patients from healthy subjects, the quantitative analysis of the disease stages requires more detailed and informative MPIs, extracted from the fine hand movements. The gait represents the most important motor task to reveal the motor impairments. However, patients at mild to moderate PD stages, do not experience significant gait disorders, contrarily to the more advanced disease stages. By definition, serious gait disorders are starting at the third HY stage and become more important at fourth and fifth HY stages. Moreover, cardinal clinical symptoms such as bradykinesia, rigidity and later the hand tremor are required for establishment of the PD diagnosis, and those symptoms are continuously present at different disease

stages. Hence, in the first three disease stages, hand movement behavior is more relevant for PD assessment and monitoring than the gait and large range upper body movements, which our results have confirmed.

The classification process for sensor glove data was performed between the groups of controls and patients (support for diagnosis) and between patients with different disease stage (support for monitoring). Three different classifiers are tested with the original feature set, six/seven most relevant features and two new features obtained from LDA (► Figure 15). Support vector machines (SVMs) are designed with the RBF kernel, whereby the bandwidth of the RBF kernel, σ varies between 0.01 and 1 and regularization parameter, C varies within a range [0.01 – 10]. K nearest neighbors classifier (KNN) is tested for the $k=1, 3$ and 5 nearest neighbors. The neural networks classifier is a multilayer perceptron with a different number of hidden layers and nodes. The parameters of classifiers are chosen from listed ranges in a validation procedure in order to achieve the highest accuracy rate. The best results on the testing set for all classifiers are obtained with the original 15D feature set. The classification accuracy is above 90% for the six/seven most relevant feature set. The lowest classification rates are reported in the case of new reduced feature space, due to the significant information losses during dimensionality reduction procedure.

These results confirm the higher informativeness of the sensor glove MPIs compared to the Kinect data MPIs and their ability to participate in both, diagnosis and monitoring evaluations of PD. Such outcome is expected, due to the high importance of hand movement analysis and quantification for PD assessment.

3.4 Correlations with Clinical Scales

We have confirmed the potential of the chosen MPIs to support the decision-making systems for diagnosis and monitoring evaluations. Another important issue is to investigate the correlation between the proposed MPIs and clinical test and scales. This is particularly important for the possible inclusion of the proposed MPIs into rehabilitation protocols. Since the clinical scales are designed for disease stage assessment, the correlation analysis is performed only for the sensor glove data MPIs.

The correlation analysis is carried out between the proposed hand MPIs (► Figure 12) and tapping test [48] and UPDRS-III clinical scale [3]. The tapping-test is performed by patients while UPDRS-III values result from the neurologist's evaluation. Correlations were calculated using Pearson's correlation coefficient r (takes values between -1 and 0 for negative correlation and between 0 and 1 for positive correlation), along with the p -value (testing the hypothesis if two variables are correlated). Scatter plots in ► Figure 16 illustrate the correlation between selected MPIs and clinical parameters, where the line represents the regression curve. It can be seen that the selected MPIs have a positive correlation with the tapping test, more concretely with the number of taps performed by the subject's right-hand palm (procedure of the tapping test is previously explained in the Section 2.2.1). This is expected since the patients who have higher values of ROM and acceleration parameter potentially can achieve a larger number of taps within defined period (30 seconds). On the other side, our MPIs have a negative correlation with the UPDRS-III scale, since the lower values of our MPIs and higher values on this scale indicate a more severe state of the patient i.e. higher disease stage.

Results of the correlation analysis have shown that some MPIs are highly correlated with both clinical parameters (11, 12, 13, 14, 24, 25 from ► Figure 12, $r > 0.5$ / $r < -0.5$, $p < 0.05$) and those MPIs represent ROM of the proximal finger joints (11–14) and velocity and acceleration parameters derived from the hand model (24, 25).

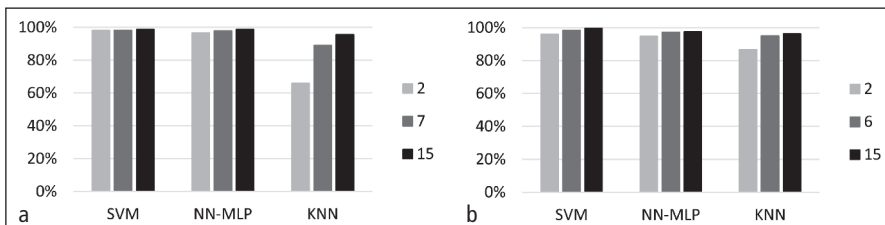


Figure 15 Classification accuracy sensor glove data: (a) patients/controls and (b) disease stages.

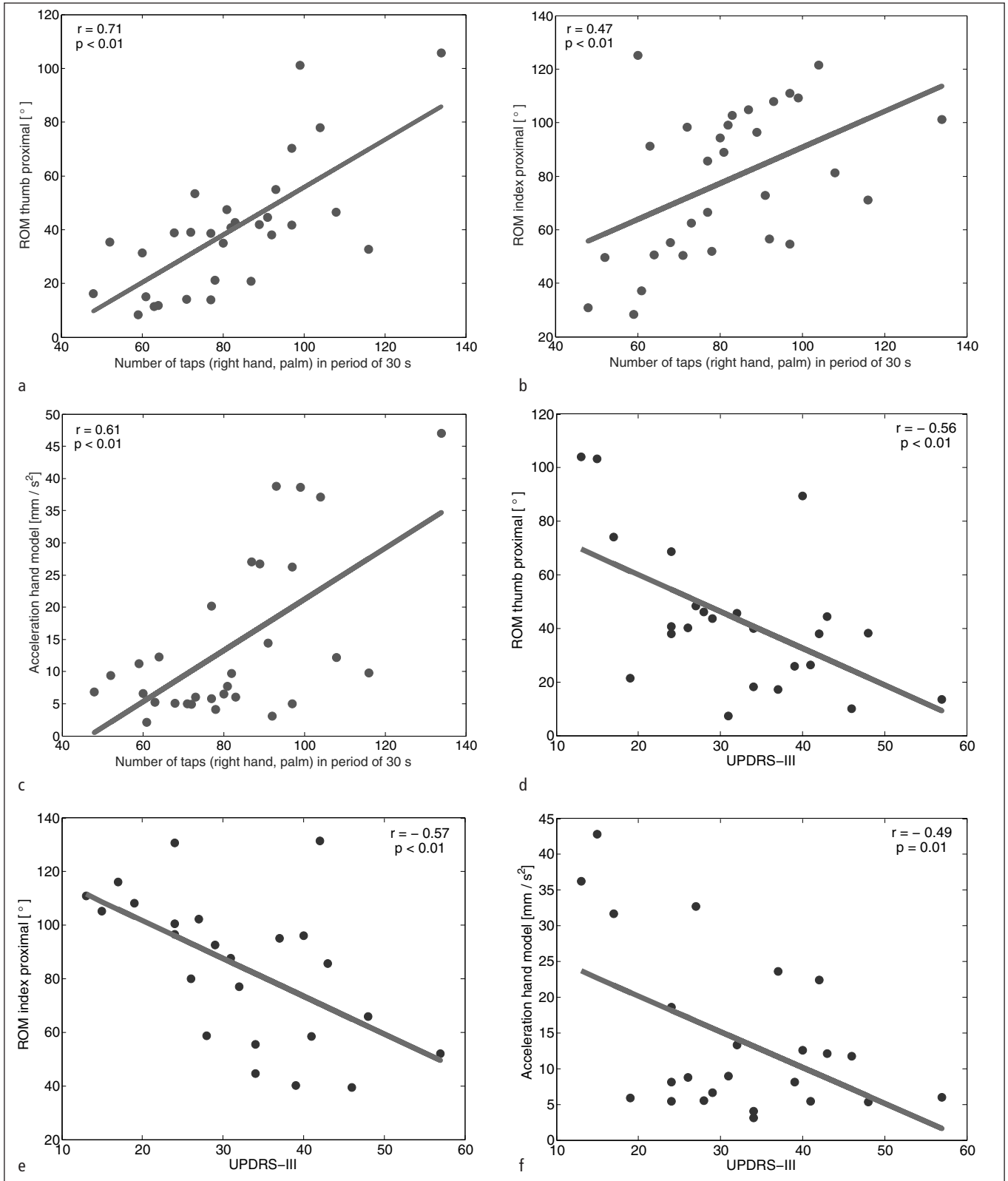


Figure 16 Scatter plots of the correlation between particular MPIs and (a–c) tapping test and UPDRS-III scale (d–f).

ROM of the metacarpal finger joints (MPIs 15, 16, 17, 18 from ►Figure 12) have shown good correlation with the tapping test ($r > 0.5$, $p < 0.05$), but not very high correlation with UPDRS-III scale ($r > -0.5$, $p > 0.05$). Angular velocity MPIs extracted from the abduction sensor data and ROM of wrist yaw are poorly correlated with both clinical parameters ($r < 0.5$ / $r > -0.5$, $p > 0.05$), except correlation of MPIs 19 and 21 (►Figure 12) with tapping test ($r > 0.5$, $p < 0.05$).

4. Discussion and Conclusions

We have presented an approach for quantitative movement analysis to support and advance traditional rehabilitation therapy, based on the full-body/hand movement data. Our results suggest that the proposed approach has the potential to be adopted by therapists, with a goal to enhance objectivity and precision, during the diagnosis and monitoring evaluations. Still, the system needs to be further tested for the validity, reliability and sensitivity to the treatment changes. At the same time, it opens the possibility of home rehabilitation for patients with the mild to moderate PD stages (I–III according to the modified HY clinical scale). Our final goal is to develop a low-cost and portable sensor system for comprehensive movement analysis in rehabilitation, suitable for home rehabilitation. In this study, data glove device has been used to test the proof of concept for the hand movement analysis, hence due to its high cost, the final version of the system, will contain alternative low-cost data glove.

We have used the Kinect device to acquire full-body movements and data glove to collect fine hand movements. We proposed a set of 25 Movement Performance Indicators (MPIs) to characterize the movements of subjects, based on the sensor data, in the context of Parkinson's disease. We conducted a thorough analysis of the properties of these MPIs, to identify the most informative in terms of assisting both the medical diagnosis and monitoring. This process unveiled the significant role of the new MPIs we proposed: (i) Kinect data – the symmetry ratio MPIs along

with the speed of the full-body movements; (ii) Sensor glove data – angular velocity MPIs extracted from the abduction sensor data and velocity and acceleration MPIs derived from the hand model, accompanying with the finger joint's range of motion. On the other hand, correlation analysis showed that the Range of Motion (ROM) of the metacarpal finger joints and velocity and acceleration parameters are correlated with clinical scales. Consequently, these MPIs satisfy important conditions for inclusion in the rehabilitation protocols – high relevance for the PD symptom assessment and important role in diagnosis and monitoring evaluations through decision-making systems. The MPIs obtained from the Kinect and data glove data were analyzed separately and can be used in different ways. The full-body MPIs are suitable to be used by therapists as a first step for the preliminary assessment of the subject's condition (detecting motor disorders). In a second step, more detailed analysis can be performed to determine the disorder severity (disease stage) using hand MPIs.

Our results have shown significant differences between patients and controls, as well as disease stages for the proposed MPIs and the possibility of successfully classifying the two conditions. The data glove sensor has proven to be more informative than the Kinect for assessing the PD main symptoms and the disease stages. This is due to the higher importance of the fine hand movement analysis, particularly for PD evaluations in comparison to the full-body movements.

In the future work, we will evaluate the system by assessing the validity, reliability and sensitivity to the treatment changes. We plan to examine the remaining group of the exercises included in the therapist's protocol – grasping and pick and place movements. Finally, we are considering using low-cost EMG sensors during those activities and to perform the movement analysis relying on the approach described in this paper.

Acknowledgment

Some parts of this study are retrieved from our previous research [21] with permission of Springer.

References

1. Jankovic J. Parkinson's disease: clinical features and diagnosis. *J Neurol, Neurosurgery and Psychiatry*. 2008; 79(4): 368–376.
2. Goetz C, Poewe W, Rascol O, et al. Movement Disorder Society Task Force report on the Hoehn and Yahr staging scale: Status and Recommendations. *Mov Disord*. 2004; 19(9): 1020–1028.
3. Goetz C, Tilley B, Shaftman S, et al. Movement Disorder Society-Sponsored Revision of the Unified Parkinson's Disease Rating Scale (MDS-UPDRS): Scale Presentation and Clinimetric Testing Results. *Mov Disord*. 2008; 23(15): 2129–2170.
4. Stamford JA, Schmidt PN, Friedl KE. What Engineering Technology Could Do for Quality of Life in Parkinson's Disease: A Review of Current Needs and Opportunities. *IEEE J Biomed Health Inform*. 2015; 19(6): 1862–1872.
5. Zhou H, Hu H. Human motion tracking for rehabilitation – A survey. *Biomed Signal Process Control*. 2008; 3(1): 1–18.
6. Parisi F, Ferrari G, Giuberti M, et al. Body-Sensor-Network-Based Kinematic Characterization and Comparative Outlook of UPDRS Scoring in Leg Agility, Sit-to-Stand, and Gait Tasks in Parkinson's Disease. *IEEE J Biomed Health Inform*. 2015; 19(6): 1777–1793.
7. Patel S, Park H, Bonato P, et al. A review of wearable sensors and systems with application in rehabilitation. *J Neuroeng Rehabil*. 2012; 9: 21.
8. Gonzalez-Jorge H, Riveiro B, Vazquez-Fernandez E, et al. Metrological evaluation of Microsoft Kinect and Asus Xtion sensors. *Measurement*. 2013; 46(6): 1800–1806.
9. Gonçalves AR, Gouveia ER, Cameirão MS, et al. Automating senior fitness testing through gesture detection with depth sensors. *IET International Conference on Technologies for Active and Assisted Living (TechAAL)*; 2015 Nov. 5; London, UK.
10. Antón D, Goñi A, Illarramendi A. Exercise Recognition for Kinect-based Telerehabilitation. *Methods Inf Med*. 2015; 54(2): 145–155.
11. Khoshelham K, Elberink S. Accuracy and resolution of Kinect depth data for indoor mapping applications. *Sensors*. 2012; 12(2): 1437–1454.
12. Clark R, Pu Y, Fortina K, et al. Validity of the Microsoft Kinect for assessment of postural control. *Gait and Posture*. 2012; 36(3): 372–377.
13. Chang C, Lange B, Zhang M, et al. Towards Pervasive Physical Rehabilitation Using Microsoft Kinect. 6th International Conference on Pervasive Computing Technologies for Healthcare (PervasiveHealth); 2012 May 21–24; San Diego, CA. pp. 159–162.
14. Chang Y, Han W, Tsai Y. A Kinect-based upper limb rehabilitation system to assist people with cerebral palsy. *Res Dev Disabil*. 2013; 34(11): 3654–3659.
15. Chang Y, Chen S, Huang J. A Kinect-based system for physical rehabilitation: A pilot study for young adults with motor disabilities. *Res Dev Disabil*. 2011; 32(6): 2566–2570.
16. Gama A, Chaves T, Figueiredo L, et al. Guidance and Movement Correction Based on Therapeutics Movements for Motor Rehabilitation Support Systems. 14th Symposium on Virtual and Augmented

- Reality (SVR); 2012 May 28–31; Rio de Janeiro, Brasil. IEEE; 2012. pp. 191–200.
17. Calin A, Cantea A, Dascalu A, et al. Mira – Upper Limb Rehabilitation System using Microsoft Kinect. *Studia Universitatis Babeş-Bolyai, Informatica*. 2011; 56 (4): 63–74.
 18. Galna B, Barry G, Jackson D, et al. Accuracy of the Microsoft Kinect sensor for measuring movement in people with Parkinson's disease. *Gait and Posture*. 2014; 39(4): 1062–1068.
 19. Galna B, Jackson D, Schofield G, et al. Retraining function in people with Parkinson's disease using the Microsoft Kinect: game design and pilot testing. *J Neuroeng Rehabil*. 2014; 11–60.
 20. Albiol-Pérez S, Lozano-Quilis J, Gil-Gómez H, et al. Virtual rehabilitation system for people with Parkinson's disease. 9th international conference on disability, virtual reality and associated technologies (ICDVRAT); 2012 Sept. 10–12; Laval, France. pp. 423–426.
 21. Spasojevic S, Santos-Victor J, Ilic T, et al. A Vision-based System for Movement Analysis in Medical Applications: the example of Parkinson's Disease. In: Nalpantidis L, Krüger V, Eklundh JO, Gastertos A, editors. *Proceedings of the 10th International Conference on Computer Vision Systems – Volume 9163 (ICVS 2015)*. New York: Springer; 2015. p. 424–434.
 22. Okuno R, Yokoe M, Akazawa K, et al. Finger Taps Movement Acceleration Measurement System for Quantitative Diagnosis of Parkinson's disease. 28th Annual International Conference of the Engineering in Medicine and Biology Society (EMBS); 2006 Aug. 30–Sept. 3; New York, NY. IEEE; 2006. pp. 6623–6626.
 23. Smeja M, Foerster, F, Fuchs, G, et al. 24-h Assessment of tremor activity and posture in Parkinson's disease by multi-channel accelerometry. *J Psychophysiol*. 1999; 13(4): 245–256.
 24. LeMoyné R, Coroian C, Mastroianni T. Quantification of Parkinson's disease characteristics using wireless accelerometers. *International Conference on Complex Medical Engineering (ICME)*; 2009 April 9–11; Tempe, AZ. IEEE; 2009. pp. 1–5.
 25. Salarian A, Russmann H, Wider, C, et al. Quantification of tremor and bradykinesia in Parkinson's disease using a novel ambulatory monitoring system. *IEEE Trans Biomed Eng*. 2007; 54(2): 313–322.
 26. Burkhard PR, Langston JW, Tetrud JW. Voluntarily simulated tremor in normal subjects. *Clin Neurophysiol*. 2002; 32(2): 119–126.
 27. Kandori A, Yokoe M, Sakoda S, et al. Quantitative magnetic detection of finger movements in patients with Parkinson's disease. *Neurosci Res*. 2004; 49(2): 253–260.
 28. Shima K, Tsuji T, Kan E, et al. Measurement and Evaluation of Finger Tapping Movements Using Magnetic Sensors. 30th Annual International Conference of the IEEE Engineering in Medicine and Biology Society (EMBS); 2008 Aug. 20–25; Vancouver, BC. IEEE; 2008. pp. 5628–5631.
 29. Shima K, Tsuji T, Kandori A, et al. Measurement and Evaluation of Finger Tapping Movements Using Log-linearized Gaussian Mixture Networks. *Sensors*. 2009; 9(3): 2187–2201.
 30. Niazmand K, Tonn K, Kalaras A, et al. Quantitative Evaluation of Parkinson's Disease using sensor based smart Glove. 24th International Symposium on Computer-Based Medical Systems (CBMS); 2011 June 27–30; Bristol, UK. IEEE; 2011. pp. 1–8.
 31. Prochazka A, Bennett DJ, Stephens MJ, et al. Measurement of Rigidity in Parkinson's Disease. *Mov Disord*. 1997; 12(1): 24–32.
 32. Hanson M, Powell H, Frysinger R, et al. Teager Energy Assessment of Tremor Severity in Clinical Application of Wearable Inertial Sensors. *IEEE/NIH Life Science Systems and Applications Workshop (LISA)*; 2007 Nov. 8–9; Bethesda, MD. IEEE; 2007. pp. 136–139.
 33. Iacono RP, Lonser RR, Maeda G, et al. Chronic Anterior Pallidal Stimulation for Parkinson's Disease. *Acta Neurochir*. 1995; 137(1–2): 106–112.
 34. Su Y, Geng D, Allen CR, et al. Three-Dimensional Motion System ("Data-Gloves"): Application for Parkinson's disease and Essential Tremor. *IEEE International Workshop on Virtual and Intelligent Measurement Systems (VIMS)*; 2001 May 19–20; Budapest, Hungary. IEEE; 2001. pp. 28–33.
 35. Su Y, Allen CR, Geng D, et al. 3-D Motion System ("Data-Gloves"): Application for Parkinson's disease. *IEEE Trans Instrum Meas*. 2003; 52(3): 662–674.
 36. Morrow K, Docan C, Burdea G, et al. Low-cost Virtual Rehabilitation of the Hand for Patients Post-Stroke. *International IEEE Workshop on Virtual Rehabilitation 2006*; New York, NY. IEEE; 2006. pp. 6–10.
 37. Lange B, Koenig S, McConnell E, et al. Interactive game-based rehabilitation using the Microsoft Kinect. *IEEE Virtual Reality Short Papers and Posters (VRW)*; 2012 March 4–8; Costa Mesa, CA. IEEE; 2012. pp. 171–172.
 38. Cho CW, Chao WH, Lin SH, et al. A vision-based analysis system for gait recognition in patients with Parkinson's disease. *Expert Syst Appl*. 2009; 36(3): 7033–7039.
 39. Lum P, Burgar C, Shor P, et al. Robot-Assisted Movement Training Compared With Conventional Therapy Techniques for the Rehabilitation of Upper-Limb Motor Function After Stroke. *Arch Phys Med Rehabil*. 2002; 83(7): 952–959.
 40. Vaisman L, Dipietro L, Krebs H. A Comparative Analysis of Speed Profile Models for Wrist Pointing Movements. *IEEE Trans Neural Syst Rehabil Eng*. 2013; 21(5): 756–766.
 41. Plamondon R. A kinematic theory of rapid human movements. Part I. Movement representation and generation. *Biol Cybern*. 1995; 72(4): 295–307.
 42. Gribble P, Ostry D. Origins of the Power Law Relations Between Movement Velocity and Curvature: Modeling the Effects of Muscle Mechanics and Limb Dynamics. *J Neurophysiol*. 1996; 76(5): 2853–2860.
 43. Bullock D, Grossberg, S. Adaptive neural networks for control of movement trajectories invariant under speed and force rescaling. *Hum Mov Sci*. 1991; 10(1): 3–53.
 44. Mirkov D, Milanovic S, Ilic D, et al. Symmetry of Discrete and Oscillatory Elbow Movements: Does it Depend on Torque That the Agonist and Antagonist Muscle can Exert? *Motor Control*. 2002; 6(3): 271–281.
 45. Available from: <http://www.cyberglovesystems.com/products/cyberglove-II/overview>.
 46. Maetzler W, Domingos J, Srulijes K, et al. Quantitative Wearable Sensors for Objective Assessment of Parkinson's Disease. *Mov Disord*. 2013; 28(12): 1628–1637.
 47. Keus S, Bloem B, Hendriks E, et al. Evidence-Based Analysis of Physical Therapy in Parkinson's Disease with Recommendations for Practice and Research. *Mov Disord*. 2007; 22(4): 451–460.
 48. Pötter-Nerger M, Wenzelburger R, Deuschl G, et al. Impact of Subthalamic Stimulation and Medication on Proximal and Distal Bradykinesia in Parkinson's Disease. *Eur Neurol*. 2009; 62(2): 114–119.
 49. Okuno R, Yokoe M, Fukawa K, et al. Measurement system of finger-tapping contact force for quantitative diagnosis of Parkinson's disease. 29th Annual International Conference of the IEEE Engineering in Medicine and Biology Society (EMBS); 2007 Aug. 22–26; Lyon, France. IEEE; 2007. pp. 1354–1357.
 50. Available from: http://petercorke.com/Robotics_Toolbox.html.
 51. Spong MW, Hutchinson S, Vidyasagar M. *Robot Modeling and Control*. John Wiley & Sons; 2006.
 52. Field A. *Discovering statistics using SPSS*. 3rd ed. London: Sage; 2009.
 53. Fisher RA. The use of multiple measurements in taxonomic problems. *Annals of Eugenics*. 1936; 7(2): 179–188.